We feel justified in presenting the ΔG values for two reasons: (1) The differences between ΔG and ΔE are dominated by the ΔS term and the compensation between the translational/rotational entropy loss and the entropy in the low frequency (<100 cm^{-1}) normal modes. There is precise information on these modes for very few molecules. Thus, calibration to experiment for these low modes would be impossible. (2) There is indirect evidence, based on a comparison of our normal mode calculations on progesterone with a variety of simple and complex force fields,[23] that such low frequency modes are relatively insensitive to details of the force field, provided that qualitatively reasonable parameters are used.

Conclusion

The major conclusions of this study are the following: (1) We have further validated the power and utility of molecular mechanical methods in simulating the kinetics and thermodynamics of ionophore–cation interactions. With use of the same set of parameters successfully applied to study 18-crown-6 (**4**), the calculations have rationalized the very different cation selectivity of **1** and **4** and the dramatically different cation affinities of **1** and **2**, as well as suggesting differences in kinetics of K^+ and Na^+ association to **1**. (2) The calculations used *no X-ray structural data*, per se, as input, illustrating the power of a distance geometry/computer graphics/molecular mechanics approach to studying molecular interactions in complex systems. A subsequent comparison of the calculated structures with the available X-ray structures of the ionophore–carbon complexes reveals satisfactory agreement, even in the case of Li^+/**3a**, where both the calculated and experimental structures find 5 short and 1 long Li···O distances. (3) The combined use of these different theoretical approaches has also enabled us to charcterize the properties of a new isomer of **3**, **3b**, which has been predicted to have the highest known Li^+ and Na^+ affinities.

(23) Kollman, P.; Murray-Rust, P.: normal mode calculations on progesterone at both the all atom and united atom level, using force field parameters from ref 6 and 9–10.

Acknowledgment. P.A.K. and G.W. are pleased to ackowledge the support of a NATO travel grant (0478/82) in this research. P.A.K. thanks Ken Trueblood for bringing these molecules to his attention, both Ken Trueblood and Donald Cram for useful comments, and the NIH (GM-29072) for research support. The facilities of the UCSF Computer Graphics Lab, supported by NIH-RR-1081 (R. Langridge, director, and T. Ferrin, system manager), were essential to the success of this study.

Note Added in Proof. R. C. Helgeson and D. J. Cram (private communication) have succeeded in preparing and characterizing **3b** and Li^+/**3b**. They have found that Li^+ is more difficult to decomplex from **3b** than from **1**, which appears to verify our prediction.

Registry No. 1a, 72526-85-3; **1b**, 95045-92-4; **2a**, 80109-06-4; **2b**, 95045-93-5; **3**, 95045-94-6; Li, 7439-93-2; Na, 7440-23-5; K, 7440-09-7.

Simulation of Formamide Hydrolysis by Hydroxide Ion in the Gas Phase and in Aqueous Solution

Scott J. Weiner, U. Chandra Singh, and Peter A. Kollman*

Contribution from the Department of Pharmaceutical Chemistry, University of California, San Francisco, California 94143. *Received May 9, 1984*

Abstract: We present the results of a new approach for simulating chemical reactions by using quantum mechanical and molecular mechanical methods. This approach is applied to the hydrolysis of formamide by hydroxide ion. In the gas phase, tetrahedral complex (TC) formation is calculated to proceed with no barrier and TC breakdown involves a small barrier (12 kcal/mol). In solution, we calculate a 22-kcal/mol barrier for *formation* of the TC with a second, smaller barrier occurring for TC breakdown. The calculated reaction energies and activation energies are in quite good agreement with available experimental data.

The mechanisms by which enzymes catalyze chemical reactions have intrigued theoretical chemists and biochemists for years.[1-4] Warshel and Levitt's pioneering approach to simulating enzymatic reactions,[5] and the application of this approach to lysozyme cleavage of saccharide linkages, was the first study which combined the environmental and internal strain factors by using a molecular mechanical model with semiempirical quantum mechanical techniques to evaluate the energetics of bond breaking. The results of their calculations were encouraging and showed the dramatic effects that electrostatic interactions have in stabilizing the intermediate carbonium ion in this reaction. Although their method has much merit, we feel that recent developments in ab initio quantum mechanical theory[6] and accurate potentials for liquid water[7] make it a propitious time to develop another approach for simulating enzymatic reactions.

With this in mind, we present a method for simulating noncatalyzed, as well as enzymatic reactions, in aqueous solution. This method can best be broken down into two very general steps: the use of ab initio quantum mechanics to evaluate bond breaking energies and molecular mechanics for calculating the remaining energies, dominated by strain and noncovalent interactions. The solute(s) is completely surrounded by explicit water molecules, taken from a Monte Carlo simulation on liquid water,[8] and allowed to energy-refine by using molecular mechanics. As our first

(1) General reviews: Walsh, C. In "Enzymatic Reaction Mechanisms"; W. H. Freeman: San Francisco, 1979. Fersht, A. In "Enzyme Structure and Mechanism"; W. H. Freeman: San Francisco, 1977.
(2) Wipff, G.; Dearing, A.; Weiner, P.; Blaney, J.; Kollman, P. *J. Am. Chem. Soc.* **1983**, *105*, 997.
(3) Scheiner, S.; Lipscomb, W. *Proc. Natl. Acad. Sci. U.S.A.* **1976**, *73*, 432.
(4) Van Duijnen, P.; Thole, B.; Hol. W. *Biophys. Chem.* **1979**, *9*, 273.
(5) Warshel, A.; Levitt, M. *J. Mol. Biol.* **1976**, *103*, 227.
(6) Binkley, J.; Whiteside, R.; Krishnan, R.; Seeger, R.; Defrees, D.; Schlegel, H.; Topiol, S.; Kahn, L; Pople, J. Gaussian BO, Indiana University, Bloomington, 1980.
(7) Jorgensen, W.; Chandrasekhar, J.; Madura, J. *J. Chem. Phys.* **1983**, *79*, 926.
(8) The Monte Carlo cube of 216 water molecules was kindly provided to us by W. Jorgensen.

0002-7863/85/1507-2219$01.50/0

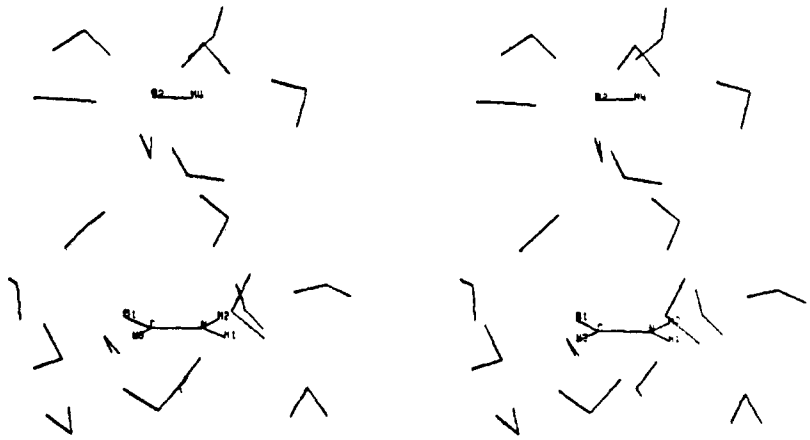

Figure 1. Stereoview of reactants at 6.00 Å after 1000 energy evaluations of molecular mechanics refinement. All solute structures were optimized at the quantum mechanical level with a 4-31G basis set.

application of this approach, we have chosen to focus on the base-catalyzed hydrolysis of formamide:

$$OH^- + H_2NCHO \rightarrow HCOO^- + NH_3 \quad (1)$$

This reaction was selected for its close analogy with amide hydrolysis catalyzed by the serine proteases:

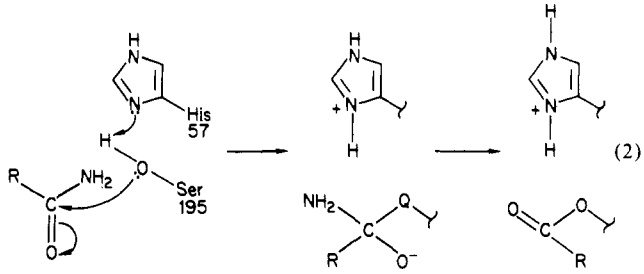

(2)

The first step in our approach uses ab initio quantum mechanical techniques for evaluating the structural, energetic, and electronic properties of various "snapshots" along the pathway of formamide hydrolysis in the gas phase.

There have been several previous ab initio studies on nucleophilic attack of carbonyl carbon centers. Alagona et al.[9] have performed ab initio minimal basis set (STO-3G) calculations on formamide bond cleavage by hydroxide in the gas phase and noted the importance of adding solvent to the calculation. A thorough quantum mechanical analysis of essentially the reverse, nonionic reaction has been performed by Oie et al.[10]

$$NH_3 + HCOOH \rightarrow NH_2CHO + H_2O \quad (3)$$

Their study focused on characterizing intermediates and transition states along the reaction pathway and showed the importance of including electronic correlation energy in the analysis of the reaction energetics.

Williams et al.[11] have extended the theory one step further by including a few ancillary solvent (water) molecules in the quantum mechanical treatment of the reaction

$$H_2O + CH_2O \rightarrow HOCH_2OH \quad (4)$$

The gas-phase mechanism was shown to be concerted and catalyzed by a single water molecule. They have shown the importance of including even a few solvent molecules into the calculation and the dramatic stabilizing effect which they can have.

These calculations, and others,[12,13] have been valuable in illustrating the power and utility of ab initio methods for studying gas-phase chemical reactions. However, realistic solvation energies can only be achieved by adding solvent into the calculation on a much larger scale. At this point there is no general agreement on the best way to proceed which is both accurate and computationally practical.[14-19]

Placing a few water molecules about the solute cannot lead to a proper evaluation of solvation energies. In particular, the disruption of water–water energies upon incorporation of ionic solutes has been shown to be very important in representing aqueous solvation; this effect is not represented in such "supermolecule" approaches. Monte Carlo[20] and molecular dynamics[21] have been applied quite successfully to studying the properties of bulk water and solvation energies of small molecules. However, these treatments are computationally very expensive for small solutes, let alone a system containing protein and substrate. It is clear that a method is needed which is capable of reasonably evaluating quantitative solvation energies, yet can be applied to enzymatic systems without using enormous amounts of computer time.

In view of the considerations mentioned above, we have combined ab initio theory with explicit solvation calculated by a molecular mechanical approach. We have performed ab initio calculations on eight "snapshot" structures along the reaction coordinate of hydroxide attack on formamide and subsequent water-catalyzed breakdown of the tetrahedral complex (TC). These gas-phase structures were placed in a solvent "bath" and energy-refined by using a molecular mechanical approach. The solvation energy of the system was then determined from these molecular mechanical calculations.

We find that in the gas phase, tetrahedral complex (TC) formation is calculated to be a "downhill" process, with the TC 26 kcal/mol lower than the reactants. A barrier of 12 kcal/mol is found for H_2O-catalyzed breakdown of the tetrahedral complex, with the products, ammonia and formate, lying 49 kcal/mol lower than the reactants. When solvent is included, a dramatic change occurred in the reaction profile. The aqueous-phase reaction is found to proceed through a solvent-induced barrier of 22 kcal/mol to TC formation, with the energetics for H_2O proton donation giving rise to a second barrier. These calculations are in qualitative agreement with experimental results[22] for hydrolysis of amides

(9) Alagona, G.; Scrocco, E.; Tomasi, J. *J. Am. Chem. Soc.* **1975**, *97*, 9876.
(10) Oie, T.; Loew, G.; Burt, S.; Binkley, S.; MacElroy, R. *J. Am. Chem. Soc.* **1982**, *104*, 6169.
(11) Williams, I.; Spangler, D.; Femec, D.; Maggiora, G.; Schowen, R. *J. Am. Chem. Soc.* **1983**, *105*, 31.
(12) Jonsson,B.; Karlstrom, G.; Wennerstrom, H.; Forsen, S.; Roos, B.; Almlof, J. *J. Am. Chem. Soc.* **1977**, *99*, 4628.
(13) Oie, T.; Loew, G.; Burt, S.; Binkley, J.; MacElroy, R. *Int. J. Quantum Chem. Quantum Biol. Symp.* **1982**, *9*, 223.
(14) Claverie, P.; Pullman, B.; Caillet, J. *J. Theor. Biol.* **1966**, *12*, 419.
(15) Beveridge, D.; Kelley, M.; Radna, R. *J. Am. Chem. Soc.* **1974**, *98*, 3769.
(16) Newton, M. *J. Chem. Phys.* **1973**, *58*, 5833.
(17) Bonaccorsi, R.; Palla, P.; Tomasi, J. *J. Am. Chem. Soc.* **1984**, *186*, 1945.
(18) Pullman, A.; Pullman, B. *Q. Rev. Biophys.* **1975**, *7*, 505.
(19) Warshel, A. *J. Phys. Chem.* **1979**, *83*, 1640.
(20) Beveridge, D.; Mezei, M.; Mehrotra, P.; Marchese, F.; Ravi-Shanker, G.; Vasu, T.; Swaminathan, S.; In "Molecular-Based Study and Prediction of Fluid Properties"; Haile, J., Mansoori, G. Eds.; American Chemical Society: Washington, DC, 1982; Adv. Chem. *Ser.* No. 191.
(21) Stillinger, F.; Rahman, A. *J. Chem. Phys.* **1974**, *60*, 1545.
(22) Guthrie, J. *J. Am. Chem. Soc.* **1974**, *96*, 3608.

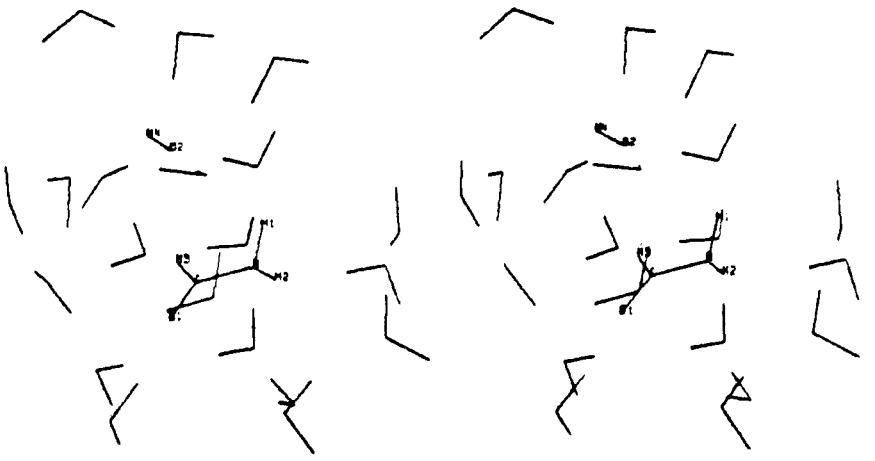

Figure 2. Same caption as Figure 1, 3.08 Å structure.

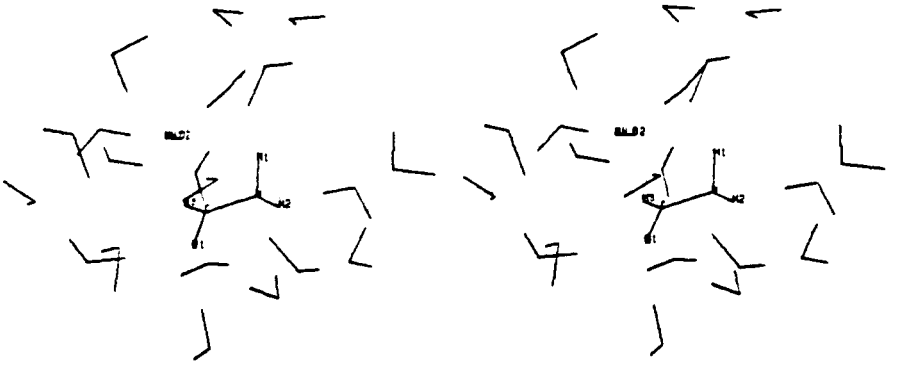

Figure 3. Same caption as Figure 1, 2.08 Å structure.

Figure 4. Same caption as Figure 1, 1.48 Å structure (TC).

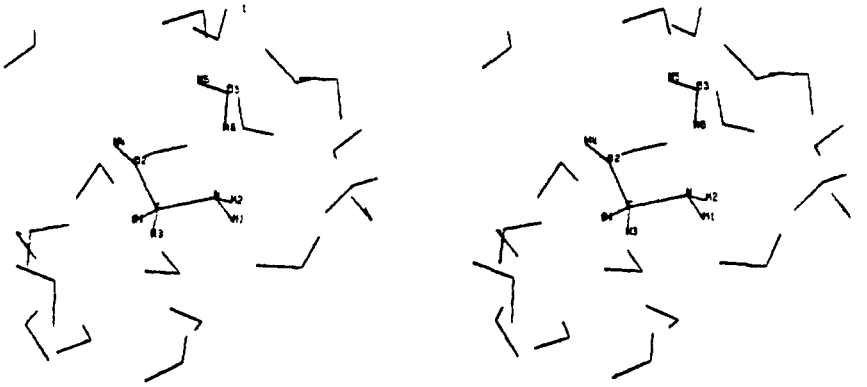

Figure 5. Same caption as Figure 1, 1.75 Å structure.

in basic solutions.

Methods

Our first goal was to simulate reaction 1 in the gas phase by using ab initio quantum mechanical techniques. We divided the reaction pathway into two parts. The first focused on OH^- attack on the carbonyl carbon of formamide and subsequent formation of a stable tetrahedral complex (Figures 1–4). We broke this part of the reaction into four distinct steps, each characterized by the distance from the hydroxide oxygen to the carbonyl carbon, the distances being 6.0, 3.08, 2.08, and 1.48 Å. The

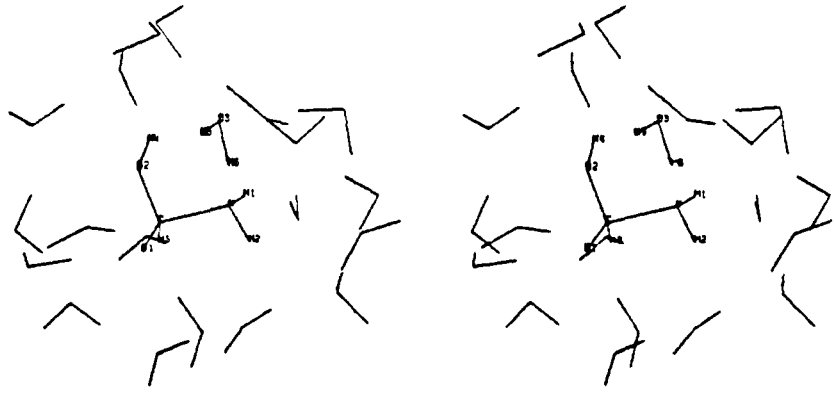

Figure 6. Same caption as Figure 1, 1.23 Å structure.

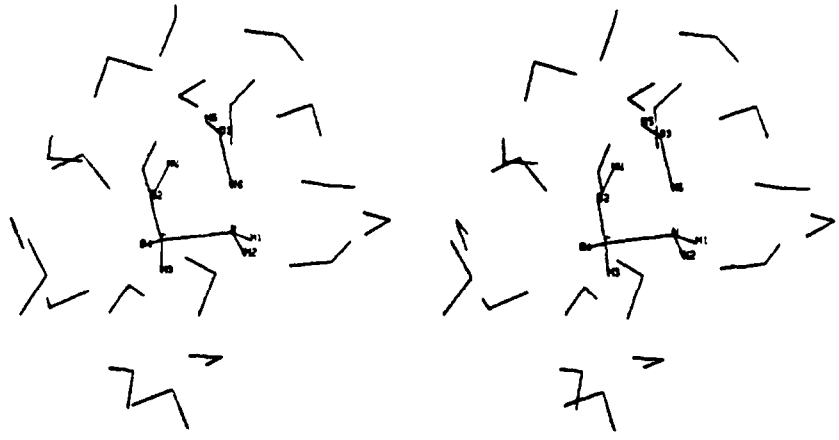

Figure 7. Same caption as Figure 1, 1.15 Å structure.

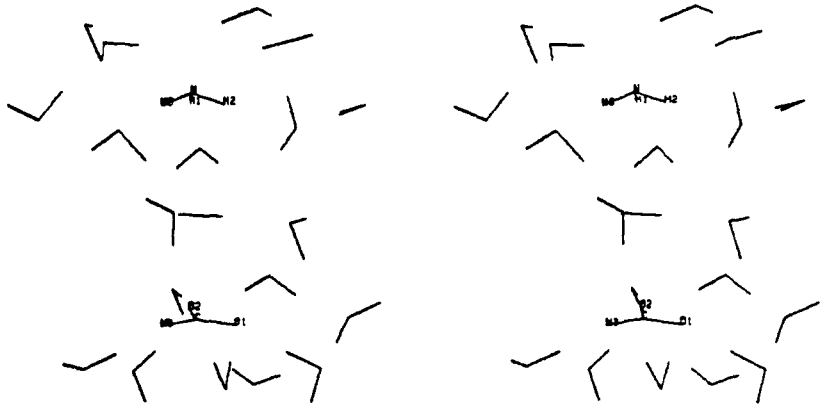

Figure 8. Same caption as Figure 1, products at 6.00 Å.

second part of the pathway represented water-catalyzed breakdown of the tetrahedral complex (Figures 5–7). Similarly, three of these snapshots are denoted by the distance between the formamide nitrogen and a hydrogen of the incoming water molecule at 1.75, 1.23, and 1.15 Å. The final geometry (Figure 8) corresponds to the products: formate and ammonia separated by 6.0 Å. All the geometries were refined by using a gradient optimization routine at the ab initio level (4-31G[23] basis set). Each degree of freedom was allowed to vary, with the sole constraint of restrained C–O (part 1) or N–H (part 2) distances. Subsequently, we carried out single point SCF 4-31 + G,[24] 6-31G*,[25] and 6-31G*/MP2[26] calculations on these eight optimized geometries to assess the effects of basis set dependence and correlation energy upon the reaction profile.

To incorporate the solvent into the calculation, we placed our quantum mechanically optimized structures within a cube of 216 water molecules. This cube was a single snapshot from a Monte Carlo simulation of pure water.[8] The starting geometries were determined by inserting the solute into the mass-weighted center of the solvent box. Any water molecular within 1.55 Å of the solute was discarded. For each of the eight structures, two or three solvent molecules were removed to accommodate the solute. The electric field generated by the solute at each water position was calculated and the water molecules reoriented, about their oxygens, by pointing the hydrogens along the direction of the target electric field component vector. Using our molecular mechanics program AMBER,[27] we energy-refined these modeled solute–solvent snapshot structures. The empirical potential energy function used appears in eq 5. The water

$$E_{tot} = \sum_{bonds} K_r (r - r_{eq})^2 + \sum_{angles} K_\vartheta (\vartheta - \vartheta_{eq})^2 + \sum_{dihedrals} \frac{V_n}{2}[1 + \cos(n_\varphi - \gamma)] + \sum_{i<j} \left[\frac{A_{ij}}{R_{ij}^{12}} - \frac{B_{ij}}{R_{ij}^{6}} + \frac{q_i q_j}{\epsilon R_{ij}} \right] + \sum_{H\,bonds} \left[\frac{C_{ij}}{R_{ij}^{12}} - \frac{D_{ij}}{R_{ij}^{10}} \right] \quad (5)$$

potentials, A_{ij}, B_{ij}, and q_i, were taken directly from the TIPS3P studies of Jorgensen.[7] Stretching and bending force constants, K_r and K_ϑ for the

(23) Hehre, W.; Stewart, R.; Pople, J. *J. Chem. Phys.* **1969**, *51*, 2657.
(24) Clark, T.; Chandrasekhar, J.; Spitznagel, G.; Schleyer, P. *J. Comput. Chem.* **1983**, *4*, 294.
(25) Hariharan, P.; Pople, J. *Theor. Chim. Acta* **1973**, *28*, 213.
(26) Binkley, J.; Pople, J. *Int. J. Quantum Chem.* **1975**, *9*, 229.
(27) Weiner, P.; Kollman, P. *J. Comput. Chem.* **1981**, *2*, 287.

water molecules were driven from a best fit of the calculated vibrational frequencies to the experimentally determined ones.[28] Values of q_i for the solute were determined by a fit of quantum mechanically generated electrostatic potential points to a point-charge model.[29] A constant dielectric constant ($\epsilon = 1$) was used. Consistent with the TIPS3P potential for H_2O–H_2O interactions, no explicit hydrogen-bonding function was evaluated. The cartesian coordinates of the solute were constrained, using a harmonic potential, with a weight of 2000 kcal/(mol Å^2), while the solute intramolecular force constants were set equal to zero. These two steps were taken to assure that the internal geometries of the solute stayed fixed to the optimized ab initio structures.

Finding a true local minimum in the solute + 216 water molecules system would only be guaranteed after achieving a large number of energy evaluations. Such a minimum would, in any case, correspond to a 0K structure. For these reasons, we chose instead to consider convergence after a fixed number of energy evaluations, to achieve not necessarily a local energy minimum, but rather a reasonable low-energy structure for each solute geometry. We eventually decided upon 1000 energy evaluations for each structure since the root mean square (rms) gradient ≈0.2 kcal/Å with the energy changing only 0.1 kcal per function evaluation in each case. More importantly, the ΔE (difference in solvation energy) *between* any two solvated structures was essentially the same after 600 and 1000 energy evaluations.

The most difficult aspect of this approach was to develop a method for accurately extracting solvation energies from the molecular mechanics refined structures. It has been shown in Monte Carlo simulations of ions in water[30] that there are two predominant energy contributions to the solvation energy of anions or small molecules, solute–solvent ($E_{\text{solute–solvent}}$) interactions and the *change* in solvent–solvent interactions upon introduction of the solute ($\Delta E_{\text{solvent–solvent}}$).

The solute–solvent interaction energy can be calculated directly from the molecular mechanical interaction energy of the solute with all the solvent molecules (most of this energy comes from waters within 4 Å of the solute). To enable us to evaluate the change in solvent–solvent energy upon introduction of the solute, $\Delta E_{\text{solvent–solvent}}$, we performed a simulation on pure water. The difficulty was in how to quantitatively extract the solvent–solvent energy from the molecular mechanics refined structures and to avoid the artifacts caused by edge effects from waters far from the solute. Given the recent results of Chandrasekhar et al.,[30] which showed that the solvent perturbation in ionic solvation is dominated by the first coordination shell, we focused on those waters in the first solvation shell, i.e., closer than the first minimum in the radial distribution function. In all cases the first minimum was well defined and there were five or six water molecules closer to the solute than this minimum. We evaluated the water–water energies for these first coordination waters and compared them with the corresponding water–water energies from the molecular mechanics optimized structure of pure water, calculated to be −24.2 kcal/mol per water molecule. $\Delta E_{\text{solvent–solvent}}$ is the difference between these.

In all of our calculations, we assumed that the total energy can be represented as a sum of three terms:

$$E_T = E_{\text{int solute}} + E_{\text{solute–solvent}} + \Delta E_{\text{solvent–solvent}} \tag{6}$$

$E_{\text{int solute}}$ represents the intrinsic energy of various solute structures taken directly from the gas-phase quantum mechanical calculations. The later two terms, $E_{\text{solute–solvent}}$ and $\Delta E_{\text{solvent–solvent}}$, can come from the molecular mechanical energies after molecular mechanics optimization on the solute in the box of water molecules. The total energy for this model, E_T(MM), is given by

$$E_T(\text{MM}) = E_{\text{int solute}}(\text{QM}) + E_{\text{solute–solvent}}(\text{MM}) + \Delta E_{\text{solvent–solvent}}(\text{MM}) \tag{7}$$

However, an alternative approach is to use this geometry and to evaluate the sum of $E_{\text{int solute}} + E_{\text{solute–solvent}}$ directly by using quantum mechanical methods.

The approach which we used for including the electrostatic environment into the quantum mechanical calculation was to represent the solvent molecules in terms of point-charges, q_i, situated at their atomic centers. These point-charges enter into the quantum mechanical calculation through the one-electron Hamiltonian as

$$\mathcal{H}_i = p_i^2 + \sum_{\text{atom}} \frac{Z_A}{r_{Ai}} + \sum_j \frac{q_j}{r_{ji}} \tag{8}$$

where j represents the atoms of the solvent system. In this manner the solute can be studied in the ab initio framework, and this energy is $E_{\text{int solute}}$ (QM + electrostatic).

In addition to the electrostatic interaction, this model also includes polarization of the solvent on the solute. To calculate the remaining polarization effects (the solute on the solvent and the solvent–solvent polarization), we used the classical method. If each atom in the solvent system is assumed to have an atomic polarizability, then the induced polarization is

$$\vec{\mu}_j = \alpha_j \vec{E}_j \tag{9}$$

where the electric field E_j on atom j is given by

$$\vec{E}_j = \sum_k^{\text{solute}} \frac{q_k \vec{r}_{ik}}{r_{ik}^3} + \sum_i^{\text{solvent}} \frac{q_i \vec{r}_{ij}}{r_{ij}^3} + \sum_{l \neq j} \vec{\nabla} \frac{\vec{\mu}_l \vec{r}_{lj}}{r_{lj}^3} \tag{10}$$

Equation 10 is solved iteratively to give the induced polarization μ_j. Only the nonbonded interactions were evaluated for the solute–solvent and the solvent–solvent. The induction energy is then given by

$$E_{\text{induction}} = -\tfrac{1}{2} \sum_k^{\text{solute}} \sum_j \frac{a_k \vec{\mu}_j \vec{r}_{kj}}{r_{kj}^3} - \tfrac{1}{2} \sum_{ij(i \neq j)}^{\text{solvent}} \frac{q_i \vec{\mu}_j \vec{r}_{ij}}{r_{ij}^3} \tag{11}$$

The point-charges for the solute were evaluated by our approach for fitting electrostatic potential points to a point-charge model.[29] The exchange interaction energy, due to solvent–solute, was calculated empirically by using a 6–12 pair potential:

$$E_{\text{nonbonded}} = \sum_{i<j} \frac{A_{ij}}{R_{ij}^{12}} - \frac{B_{ij}}{R_{ij}^6} \tag{12}$$

Thus, we can estimate the sum $E_{\text{int solute}} + E_{\text{solute–solvent}}$ by the three terms $E_{\text{int solute}}$ (QM + electrostatic) + $E_{\text{induction}}$ + $E_{\text{nonbonded}}$, even though $E_{\text{induction}}$ contains both solute–solvent and solvent–solvent polarization. However, it does not contain the term that is most difficult to determine, the differences in water–water interactions upon perturbation by the solute, $\Delta E_{\text{solvent–solvent}}$. These water–water interactions have been calculated with the molecular mechanical approach described above. This leads to an alternate formulation of the energy system E_T(QM):

$$E_T(\text{QM}) = E_{\text{int solute}}\ (\text{QM} + \text{electrostatic}) + E_{\text{induction}} + E_{\text{nonbonded}} + \Delta E_{\text{solvent–solvent}}(\text{MM}) \tag{13}$$

All of the simulations were performed on the U.C.S.F. Structural Biology VAX-11/780 and the structures displayed on the U.C.S.F. Computer Graphics Lab Evans and Sutherland Picture System.

Results

(A) Formation of the Tetrahedral Complex. Our first focus will be on the quantum mechanical and molecular mechanical results for the steps leading up to tetrahedral complex formation. We have modeled the four initial snapshot structures to be representative of reasonable steps along the pathway of OH^- attack. The starting distance of 6.0 Å between hydroxide ion and formamide was selected since it is long enough for the reactants to be considered as essentially separated species, yet small enough for each molecule to be completely solvated within a single cube of 216 Monte Carlo water molecules. The structure of the 1.48-Å complex was determined by complete relaxation of *all* parameters during the ab initio optimization, with the 2.08- and 3.08-Å structures being logically selected intermediates and optimized with respect to the fixed O2–C distance.

We optimized formamide and hydroxide at the 4-31G level and then carried out a single point ab initio calculation, using these internal geometries, for the reactants separated by 6.0 Å. After optimization of the 3.08-Å structure, the hydroxide ion was found to have migrated over toward the nitrogen end of formamide and to have abstracted one of the amide protons, forming $CHONH^-$ + H_2O. We found this complex as the lowest energy structure on the gas-phase potential surface, −29 kcal/mol relative to the tetrahedral complex. The structure corresponded to a hydrogen bond between the water and formamide anion. This is qualitatively consistent with the expectation[31] that $CHONH^-$ + H_2O is more

(28) Shimanouchi, T. In "Tables of Molecular Vibrational Frequencies"; National Standard Reference Data Series-National Bureau of Standards: Washington, DC, 1967; Parts 1-3.

(29) Singh, U. C.; Kollman, P. *J. Comput. Chem.* **1984**, *5*, 129.

(30) Chandrasekhar, J.; Spellmeyer, D.; Jorgensen, W. *J. Am. Chem. Soc.* **1984**, *106*, 903.

(31) The proton affinity of OH^- is 390 kcal/mol; that of $HCONH^-$ is likely to be similar to that of $HCOO^-$ (342 kcal/mol). This difference in anion stabilities will dominate any differences in bond energies and make $HCONH^-$ + H_2O much more stable than $HCONH_2$ + OH^-. Kebarle, P. *Annu. Rev. Phys. Chem.* **1977**, *27*, 235.

Table I. Energies for the Quantum Mechanical Model for Hydroxide Attack[a]

	gas phase[b]			solution[c]		
struct[d]	4-31G	6-31G*	6-31G*/MP2	4-31G	6-31G*	6-31G*/MP2
reactants	0.0[e]	0.0[f]	0.0[g]	0.0[h]	0.0[i]	0.0[j]
3.08	−20.4	−21.2	−22.2	22.6	22.7	21.7
2.08	−28.5	−27.3	−34.6	38.6	40.9	35.8
1.48 (TC)	−38.9	−39.8	−46.6	38.4	40.0	34.5

[a] All energies are relative to the reactants. [b] Ab initio quantum mechanical calculations ($E_{\text{int solute}}$) (kcal/mol). [c] Ab initio quantum mechanical calculations incorporating the electrostatic, polarization, and nonbonded energies of the solvent into the calculation ($E_{\text{int solute}} + E_{\text{solute-solvent}}$) (kcal/mol). [d] Notation for the structures appears in Figures 1-4. [e] Total quantum mechanical energy is −243.910 61 au. [f] Total quantum mechanical energy is −244.255 02 au. [g] Total quantum mechanical energy is −245.905 14 au. [h] Total quantum mechanical energy is −244.309 97 au. [i] Total quantum mechanical energy is −244.653 46 au. [j] Total quantum mechanical energy is −245.300 45 au.

stable than $H_2NCHO + OH^-$ in the gas phase. Hence, we did not completely gradient optimize the 3.08-Å structure (with only the C–O distance constraint) but stopped the optimization after ten cycles, in order to assure that the OH^- was in an intermediate position for attack on the carbonyl carbon. The 2.08- and 1.48-Å geometries each took ≈35–40 cycles of optimization before the largest component of the gradient was less than 0.003 au. To better assess the basis set dependence on the energetics of the four structures, we subsequently performed single-point ab initio quantum mechanical calculations on the 4-31G optimized geometries by using a 6-31G* basis set. Møller–Plesset perturbation theory at the second-order level (MP2) was also used to estimate the correlation energy and the effect which they may have on stabilizing intermediates or transition states along the pathway. The gas-phase quantum mechanical results for hydroxide attack appear in Table I.

As can be seen from Table I, both basis sets suggested that the energy of the system for OH^- attack on NH_2CHO monotonically decreased throughout. The ΔE for this half of the reaction was −38.9 kcal/mol (4-31G), and the 4-31G energies were similar to the 6-31G* over this part of the reaction. When MP2 correlation energy is included, the 1.48- and 2.08-Å structures are stabilized by ≈6.5 kcal/mol relative to the 3.08- and 6.00-Å geometries. Although in solution the tetrahedral complex might be expected to correspond to a high-energy transition state, in the gas phase this structure is energetically much more stable than the reactants. Upon approach of the hydroxide ion, the C–N bond begins to lengthen from 1.34 to 1.47 Å and the hybridization of both the carbon and the nitrogen atoms changes from sp^2 to one having more sp^3 character (Figure 1–4). The amide protons can be seen to flip up, out of the plane, consistent with the tendency for the nitrogen lone pair to be antiperiplanar to the C–O bond.[32]

The four optimized structures were placed in a water bath and restrained to their starting geometries, and the water structure was energy-refined with 1000 energy evaluations of conjugate gradient minimization. After the molecular mechanics refinement, each of these systems was found to have a relatively strong hydrogen-bonding network for the solvent structure and a well-defined first coordination shell (Figures 1–4).

We wished to assess whether the solvation properties of the various structures made physical sense. We thus analyzed the number and geometry of the water molecules forming hydrogen bonds with the solute atoms (Table II). Some points are worth noting. First, over the course of the first part of the reaction, the distance of the water hydrogens interacting with the nitrogen decreases as the hydroxide approaches. This is consistent with the fact that in the 6.0-Å structure, the nitrogen is an amide which is a rather poor hydrogen bond acceptor. Upon attack by OH^-, the nitrogen begins to take on more amine character and becomes a much better hydrogen bond acceptor. Second, in the 6.0-Å structure, there are six water molecules forming hydrogen bonds, with distances ranging from 1.62 to 1.72 Å, about the hydroxide (O2). As the reaction approaches the tetrahedral complex, with the subsequent transfer of charge from hydroxide to formamide, the total number of hydrogen bonds about the oxygen (O2) decreases to two, with only one of these a strong, near-linear H bond. Third, the number and (inferentially) strength of hydrogen bonding to the formamide oxygen increases during the course of the reaction, as O1 takes on more negative ion character. However, the hydroxide hydrogen has little tendency to hydrogen bond because it bears too little positive charge. Finally, the amide hydrogens both form reasonable H bonds in the 6.00-Å structure but not for the tetrahedral complex, consistent with amides being better hydrogen bond donors than amines.

Table II. Solute–Solvent Hydrogen-Bonding Geometries (Distance and Angle)[a]

	complexes			
atom	6.00 (react.)	3.08	2.08	1.48 (TC)
formamide H1	2.36 (136)	1.76 (158)	2.29 (164)	
formamide N			2.21 (147)	2.18 (143)
formamide H2	1.92 (174)		2.22 (139)	
formamide O1		1.60 (170)	1.61 (176)	1.55 (174)
			1.72 (166)	1.56 (166)
			2.22 (129)	1.57 (172)
hydroxide O2	1.62 (177)	1.51 (179)	1.66 (169)	1.77 (166)
	1.62 (175)	1.58 (175)	1.68 (171)	2.17 (127)
	1.65 (171)	1.59 (171)	1.89 (152)	
	1.66 (179)	1.62 (164)	2.17 (151)	
	1.66 (170)			
	1.72 (171)			
hydroxide H4	2.26 (106)	2.22 (102)	2.38 (105)	
	2.37 (93)	2.31 (95)		

[a] The structures appear in Figures 1–4. The hydrogen bond distance (in Å) is measured from water proton/oxygen to solute acceptor/donor atom. The angle is defined by hydrogen donor–acceptor (in deg). All H-bond distances less than 2.4 Å are reported.

Table III summarizes the values for the solvation energy calculated at the molecular mechanical level. It is clear that the solvent dramatically changes the energy profile of the first part of the reaction relative to the gas-phase values. The solute–solvent energy is strongest for the separated reactants, much more so than either of the other three structures. Perturbations of the solvent in the first shell were also found to be greatest for the reactants, where the highly negative hydroxide ion strongly interacts with six water molecules. Here the $\Delta E_{\text{solvent-solvent}}$ is 71.7 kcal/mol relative to pure water. The other three structures have $\Delta E_{\text{solvent-solvent}}$ ranging from 40.5 to 49.6 kcal/mol. The net effect is 42 kcal/mol of stabilization of separated reactants over the tetrahedral complex due to solvation.

We also used quantum mechanical methods to estimate $E_{\text{int solute}} + E_{\text{solute-solvent}}$ by carrying out ab initio calculations as described in the Methods section. In Table III, we compare this sum to the corresponding values from the combined quantum mechanical and molecular mechanical approach. As one can see, the two sets of energies give a very similar reaction profile.

(B) Water-Catalyzed Breakdown of the Tetrahedral Complex. The second part of the reaction is water-catalyzed breakdown of the tetrahedral complex to formate and ammonia. There are two ways that TC breakdown can occur: (1) direct donation of the internal proton (H4) to the nitrogen with concurrent C–N bond breakage and (2) water-mediated proton donation to the nitrogen. Williams et al.[11] have shown that, in the gas phase, a single ancillary water molecule lowered the barrier by 41 kcal/mol for the hydrolysis of formaldehyde. For this reason, we expect that water-mediated proton transfer will be more favorable than direct donation. Thus, we have added a single water molecule into the quantum mechanical tetrahedral complex and have optimized this structure at the 4-31G level followed by single-point ab initio calculations at the 4-31+G, 6-G*, and 6-31G*/MP2 levels. This

(32) Lehn, J.; Wipff, G. *J. Am. Chem. Soc.* **1980**, *102*, 1347.

Table III. Energies for the Molecular Mechanics Model for Hydroxide Attack

struct[a]	H_2O[b]	$E_{solute-solvent}$[c]	$\Delta E_{solvent-solvent}$[d]	$E_{solvation}$[e]	$\Delta E_{solvation}$[f]	ΔE(MM)[g]	ΔE(QM)[h]
react	6	−231.5	71.7	−159.8	0.0	0.0	0.0
3.08	5	−185.9	49.6	−136.3	23.5	23.4	21.7
2.08	6	−157.2	40.6	−116.6	43.2	39.7	35.8
1.48 (TC)	5	−158.0	40.5	−117.5	42.3	26.9	34.5

[a] The structure appear in Figures 1–4. [b] The number of water molecules in the first shell. The first shell is defined as those waters found with oxygen distances less than the first minimum in the radial distribution function of solute–water (oxygen). [c] Molecular mechanics nonbonded (van der Waals + electrostatic) energy due to solute–solvent interactions (kcal/mol). [d] Energy difference between the water molecules in the first shell and an equivalent number of "ideal" water molecules. An ideal water here has an interaction energy of −24.2 kcal/mol. [e] $E_{solute-solvent} + \Delta E_{solvent-solvent}$ (kcal/mol). [f] Same as *e* but relative to the reactants (kcal/mol). [g] Gas-phase quantum mechanical energy of the optimized structures at the 6-31G*/MP2 level with molecular mechanics solute solvent energy; $E_{int\ solute}$(QM) + $E_{solute-solvent}$(MM) (kcal/mol). [h] 6-31G*/MP2 quantum mechanical calculations incorporating the electrostatic environment; $E_{int\ solute}$(QM + electrostatic) + $E_{induction}$ + $E_{nonbonded}$ (kcal/mol).

Table IV. Energies for the Quantum Mechanical Model for Water-Catalyzed Hydrolysis[a]

	gas phase[b]			solution[c]		
struct[d]	4-31G	6-31G*	6-31G*/MP2	4-31G	6-31G*	6-31G*/MP2
1.75	0.0[e]	0.0[f]	0.0[g]	0.0[h]	0.0[i]	0.0[j]
1.23	13.0	17.0	9.8	10.9	13.9	6.7
1.15	14.2	19.8	12.2	8.6	13.8	6.1

[a] All energies are relative to the reactants (kcal/mol). [b] Ab initio quantum mechanical calculations ($E_{int\ solute}$) (kcal/mol). [c] Ab initio quantum mechanical calculations incorporating the electrostatic, polarization and nonbonded, energies of the solvent into the calculation ($E_{int\ solute} + E_{solute-solvent}$) (kcal/mol). [d] Notation for the structures appears in Figures 5–7. [e] Total quantum mechanical energy is −319.905 59 au. [f] Total quantum mechanical energy is −320.349 04 au. [g] Total quantum mechanical energy is −321.196 80 au. [h] Total quantum mechanical energy is −320.179 97 au. [i] Total quantum mechanical energy is −320.614 32 au. [j] Total quantum mechanical energy is −321.462 08 au.

structure is shown in Figure 5 and is labeled 1.75 Å to correspond to the distance between the water hydrogen (H6) and nitrogen. The water proton was then forced to move to 1.23 and 1.15 Å from the nitrogen. At each point the ab initio energies were optimized by using gradient methods.

Figures 5–7 illustrate the geometry of these gas-phase gradient-optimized structures. Figure 5 shows the water molecule forming a hydrogen bond, 1.75 Å, with the nitrogen of the tetrahedral complex. As this hydrogen is being donated to the recipient nitrogen, Figures 5–7 show a concurrent breaking of the C–N bond, with the distance going from 1.51 to 1.77 Å through these three steps. Interestingly, the hydroxyl hydrogen (H4) is found to remain bound to the oxygen throughout these three steps (0.99 Å when N–H = 1.15 Å). As the reaction proceeds, H4 was found to swing around and form an H bond with the eventual recipient water oxygen, O3 (H bond = 1.77 Å in Figure 7). We carried out further gradient optimization and found this consistent with abstraction of H4 by the water *after* the C–N distance had reached 2.0 Å. By this point, the quantum mechanical energy was much lower than the 1.15-Å structure, so the transition state for this step seems to occur near the 1.23-Å structure. These results imply that, in the gas phase, tetrahedral complex breakdown is a stepwise process: beginning first with H_2O proton donation to the nitrogen and followed by proton transfer from the tetrahedral complex to the recipient water oxygen. Also in Figure 5, one sees that the N lone pair has inverted from the structure of TC and is now no longer antiperiplanar (app) to the C–O bond. This lone pair inversion prior to the H4 → N transfer was also found in the calculations by Alagona et al.[9] They found that H4 transfer to N without water catalysis involved an ≈35 kcal/mol barrier. Without N inversion, the barrier would certainly have been larger both in our calculations and those of Alagona et al.[9]

The quantum mechanical energies are summarized in Table IV. Focusing only on the first three steps, the barrier for proton donation (over the distance 1.75–1.15 Å) is 14.2 kcal/mol (4-31G), 19.8 kcal/mol (6-31G*), and 12.2 kcal/mol (6-31G*/MP2).

The molecular mechanics hydrogen-bonding geometries and refined energies are summarized in Tables V and VI, respectively. In the 1.75-Å structure, the catalytic water oxygen (O3) is forming

Table V. Solute–Solvent Hydrogen-Bonding Geometries (Distance and Angle)[a]

	complexes			
atom	1.75	1.23	1.15	products[b]
amine		2.27 (146)	2.29 (135)	1.90 (158)
H1			2.32 (136)	
amine				2.14 (137)
N				2.15 (136)
amine		2.33 (149)		2.22 (134)
H2				
water O3	1.80 (156)	1.68 (175)	1.61 (175)	x
	1.86 (154)	1.72 (162)	1.72 (151)	x
			1.75 (166)	x
water H5				x
water H6			2.26 (144)	x
formate	1.62 (167)	1.56 (177)	1.61 (187)	1.53 (176)
O1	1.62 (167)	1.59 (178)	1.64 (162)	1.62 (178)
		1.69 (164)	1.67 (168)	
formate	1.68 (171)	1.87 (149)	1.80 (145)	1.60 (172)
O2				1.76 (172)
				1.80 (165)
				1.99 (159)

[a] The structures appear in Figures 5–8. The hydrogen bond distance (in Å) is measured from water proton/oxygen to solute acceptor/donor atom. The angle (in deg) is defined by hydrogen donor–acceptor (in deg). All H-bond distances less than 2.4 Å are reported. [b] Products are separated by 6.0 Å. See Figure 8. (For only the product structure, the water atoms (O3, H5, and H6) are no longer treated in the quantum mechanical model, and, hence, we report no hydrogen bond values for these atoms in the table.)

two hydrogen bonds (1.80 and 1.86 Å). As the reaction proceeds and the proton (H6) is donated to the nitrogen, this same oxygen forms three strong hydrogen bonds (1.61, 1.72, and 1.75 Å) with the solvent. It is not until the C–N bond is completely broken, and the products are released, that the nitrogen is "freed" for forming hydrogen bonds. This is illustrated in Table V where it is shown that no solvent molecules are closely associated with the nitrogen until ammonia is created. Both O1 and O2 are highly solvated over all the modeled reaction steps, with the number and the quality of the hydrogen bonds increasing to a maximum when the anionic formate is formed. The two formate oxygens are solvated by six water molecules, all with distances less than 1.99 Å. Figure 8 illustrates the solvated products (NH_3 + $HCOO^-$).

In contrast to OH^- attack, the molecular mechanics solute–solvent energies (Table VI) for the second part of the hydrolysis are very similar for each of the three structures. This is consistent with the fact that one has a relatively large, diffuse anion throughout the reaction.

(C) Entire Reaction Profile. At this point we assess our methods for calculating $E_{int\ solute}$. By carrying out calculations on OH^-, H_2O, $HCOO^-$, and HCOOH with the 4-31G and 6-31G* basis sets, both with and without MP2 correlation correction, we find that all these levels of theory overestimate the proton affinity of OH^- by ≈35 kcal/mol and that of formate by ≈15 kcal/mol. Such large differential errors are unsatisfactory, particularly for comparing the energy of small anions like OH^- and large diffuse ions like the tetrahedral intermediate.

Fortunately, Clark et al.[24] have shown that ab initio calculations performed with an augmented 4-31G basis set (4-31+*G*) gave

Table VI. Energies for the Molecular Mechanics Model for Tetrahedral Breakdown

struct[a]	H_2O[b]	$E_{solute-solvent}$[c]	$\Delta E_{solvent-solvent}$[d]	$E_{solvation}$[e]	$\Delta E_{solvation}$[f]	ΔE(MM)[g]	ΔE(QM)[h]
1.75	6	−143.5	41.8	−101.7	0.0	0.0	0.0
1.23	6	−156.7	58.5	−98.2	3.5	−3.4	6.7
1.15	6	−155.0	36.9	−118.1	−16.4	0.7	6.1

[a] Notation for the structures appears in Figures 5–7. [b] The number of water molecules in the first shell. The first shell is defined as those waters found with oxygen distances less than the first minimum in the radial distribution function of solute–water (oxygen). [c] Molecular mechanics nonbonded (van der Waals + electrostatic) energy due to solute–solvent interactions (kcal/mol). [d] Energy differences between the water molecules in the first shell and an equivalent number of "ideal" water molecules. An ideal water here has an interaction energy of −24.2 kcal/mol. [e] $E_{solute-solvent}$ + $\Delta E_{solvent-solvent}$ (kcal/mol). [f] Same as *e* but relative to the reactants (kcal/mol). [g] Gas-phase quantum mechanical energy of the optimized structures at the 6-31G*/MP2 level with molecular mechanics solute–solvent energy; $E_{int\ solute}$(QM) + $E_{solute-solvent}$(MM) (kcal/mol). [h] 6-31G*/MP2 quantum mechanical calculations incorporating the electrostatic environment; $E_{int\ solute}$(QM + electrostatic) + $E_{induction}$ + $E_{nonbonded}$ (kcal/mol).

Table VII. Energies for the Separated Reactants and Products

struct	6-31G*/MP2[a]	4-31+G[b]	4-31+G+CF[c]	$E_{solute-solvent}$[d]	$E_{solvent-solvent}$[e]	ΔE[f]
OH^-	−75.513 13	−75.289 90		−173.7	34.0	
$HCONH_2$	−169.392 97	−168.692 38		−20.3	8.5	
NH_3	−56.348 48	−56.114 99		−15.2	8.6	
$HCOO^-$	−188.667 25	−187.932 66		−146.0	39.8	
react[g]	0.0	0.0	0.0	0.0	0.0	0.0
prod[g]	−68.8	−41.0	−48.9 (−46.3)	32.8	5.9	−10.2 (−5.2)

[a] Absolute quantum mechanical energies with a 6-31G*/MP2 basis (in au). [b] Absolute quantum mechanical energies with 4-31+G basis (in au). [c] Relative 4-31+G energies + correction factor (CF). CF is defined as the energy difference between reactants and products calculated with a 4-31G and 6-31G*/MP2 model. Experimental gas-phase value appears in parentheses (ref 34) (kcal/mol). [d] Molecular mechanics $E_{solute-solvent}$ (kcal/mol). [e] Molecular mechanics $\Delta E_{solvent-solvent}$ (kcal/mol). [f] "Best" estimate of the energy of reaction in aqueous solution. 4-31+G + CF + $E_{solute-solvent}$ + $\Delta E_{solvent-solvent}$. Experimental aqueous phase value appears in parentheses (ref 35) (kcal/mol). [g] Relative energy of reactants and products (kcal/mol).

excellent agreement with experiment for the proton affinities of OH^- and $HCOO^-$, within 5 and 2 kcal/mol, respectively. We have thus performed single-point ab initio calculations on each of the eight gradient-optimized structures by employing this augmented 4-31+G basis set. Single diffuse p and sp functions were added to each heavy atom in line with the exponents reported by Clark et al.[24]

We can also use the 4-31+G basis set to calculate a ΔE for reaction 1 in the gas phase and solution (Table VII). We assume that both the 4-31+G and 6-31G*/MP2 models are better than 4-31G and that each is "correcting" different defects in the more limited 4-31G model. Thus, our "best" quantum mechanical energies are the 4-31+G values plus the energy difference between 4-31G and 6-31G*/MP2. To these quantum mechanical energies we have added the solvation energies calculated as described above (using the first shell waters to estimate the change in solvent–solvent energy). As one can see, both the ΔE_T calculated for this reaction in the gas phase and in solution are in encouraging agreement with experiment and support the use of this approach for evaluating the energies along the reaction pathway.

Table VIII summarizes our best values for the various energies and energy components. Because the diffuse functions in the 4-31+G basis set give large counterpoise errors[33] for intermediate (partially bonded) structures, we used the 4-31+G energies only to estimate the energies for the reactants (6.0 Å) and the TC. We confirmed that there was negligible counterpoise error in the 6.00-Å (4-31+G) calculations by comparing its total energy with the same reactants separated at infinity. The 2.08- and 3.08-Å energies were scaled between the 6.00- and 1.48-Å (TC) energies in the same proportion as found at the 6-31G*/MP2 levels. We then added the difference between 4-31G and 6-31G*/MP2 energies to these 4-31+G values to arrive at our best estimate of the quantum mechanical energies for these structures as we had done for the overall reaction ΔE (Table VII). In the second part of the reaction, we used the 6-31G*/MP2 energies as our best estimate, since these structures are all similar, diffuse anions and the proton affinity error will not be so large.

As a final step in the analysis, we wished to compare the energy of the TC (the final structure of the first part of the reaction profile) and that of 1.75-Å structure, which has been created by ab initio gradient optimization of 1.48 Å with an additional water hydrogen bonding to the nitrogen (the first structure of the second part of the reaction). We do this in the following way: to the molecular mechanics solute–solvent energy of 1.75 Å (−143.5 kcal/mol) we add the 6-31G*/MP2 ab initio calculated energy lowering due to the water–tetrahedral intermediate interaction (the energy difference between the 1.75-Å structure + an infinitely separated water vs. the 1.48-Å structure), which is 14.0 kcal/mol. This gives a net water–tetrahedral intermediate solute–solvent interaction energy (where the quantum mechanical water has been included with the classical waters) of −157.5 kcal/mol, essentially identical with that of the 1.48-Å solute–solvent energy of −158.0 kcal/mol. However, the five waters in the first coordination shell of the 1.48-Å structure have a $\Delta E_{solvent-solvent}$ of −80.5 kcal/mol, and the four classical waters and the one quantum mechanical water of the 1.75 Å have $\Delta E_{solvent-solvent}$ = −89.7 kcal/mol, leading to a net stabilization of 1.75 Å, relative to 1.48, of 8.7 kcal/mol. Thus in Figure 9, we use the values in Table III plus the estimated energy difference between 1.48 and 1.75 Å to describe a complete reaction profile for gas-phase and aqueous hydrolysis of formamide.

Table VIII. Reaction Pathway Energies in the Gas Phase and in Solution

struct[a]	4-31+G[b]	CF[c]	ΔE(gp)[d]	ΔE(aq)[e]
react	0.0	0.0	0.0	0.0
3.08	−9.9	−1.8	−11.7	11.8
2.08	−15.4	−6.1	−21.5	21.7
1.48	−18.9	−7.4	−26.3	16.0
1.75			−40.3	8.7
1.23			−30.5	22.0
1.15			−28.1	4.4
prod			−48.9	−10.2

[a] Structures appear in Figures 1–7; product energies taken for the infinitely separated species and not the configuration shown in Figure 8. [b] Quantum mechanical energies with 4-31+G basis (kcal/mol). [c] Correction factor for correlation energy, taken as the energy difference between each structure calculated with a 4-31G and 6-31G*/MP2 model (kcal/mol). [d] Our "best" estimate of the gas-phase reaction. For part 1 and the products we used 4-31+G+CF. For the three steps in part 2 we used 6-31G*/MP2 (kcal/mol). [e] Our "best" estimate of the aqueous-phase reaction. To the $E_{int\ solute}$ (ΔE(gp)), we add $E_{solute-solvent}$(MM) + $\Delta E_{solvent-solvent}$(MM) (kcal/mol).

Discussion

We first wish to assess the accuracy of the gas-phase and solution-phase reaction energies presented in Figure 9. There are four experimental points which we can compare with our calcu-

(33) Boys, S.; and Bernardi, F. *Mol. Phys.* **1970**, *19*, 558.

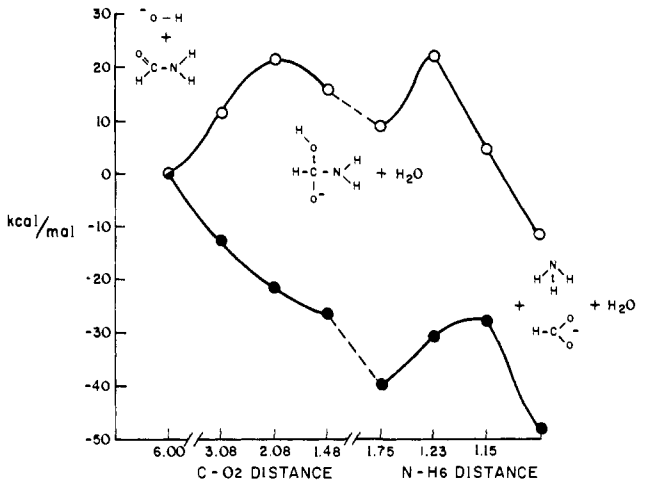

Figure 9. Representation of reaction coordinate (ordinate) for gas phase (solid circles) and aqueous phase (open circles) of the formamide hydrolysis reaction. The relative energy values are taken from Table VIII. The gas-phase and aqueous-phase energies are set equal to each other at 6.00 Å in order to better compare the energy profiles. The strucures represented on the figure depict reactants, transition state, and products, respectively. The points on the abscissa represent the structures in Figures 1-8. They are equally spaced only for representational purposes.

lated values. First, the experimental ΔH for $H_2NCHO + OH^- \rightarrow NH_3 + HCOO^-$ in the gas phase can be compared with the results of our quantum mechanical calculations. The ΔH_{exptl} = −46.3 kcal/mol (ref 34) is in very good agreement with ΔE_{QM} = −48.9 kcal/mol. Secondly, the experimental solution-phase enthalpy ΔH = −5.2 kcal/mol (ref 35) can be compared with the two endpoints in Figure 9 and is found to be in reasonable agreement with the calculated ΔH = −10.2 kcal/mol. Thirdly, kinetic isotope effect experiments on base-catalyzed hydrolysis of amides[36] are consistent with the rate of hydrolysis (k_h) being nearly equal to the rate of ^{18}O exchange (k_e). This result implies that the energy difference between the first barrier and TC is nearly equal to the energy difference between the second barrier and TC. This is consistent with our calculated energy differences of 13.0 and 13.3 kcal/mol, respectively. Finally, it is encouraging that the calculated barrier reported here is quite consistent with the thermodynamic analysis of Guthrie[22] on base-catalyzed hydrolysis of amides. Guthrie suggests an effective $\Delta G^{\ddagger} \approx 22$ kcal/mol for amide hydrolysis, consistent with our calculated $\Delta E^{\ddagger}$ of 22.0 kcal/mol.

The encouraging agreement of calculated and experimental energies supports our assumed mechanism for the reaction, although it does not prove it. In the (hypothetical) gas-phase reaction, OH^- attack proceeds without a barrier but the second step, water-catalyzed proton transfer, involves a barrier of 12 kcal/mol. In solution, on the other hand, there is a solvent-induced barrier to OH^- attack, due to the more favorable solvation of OH^- than the more diffuse anions on the pathway to tetrahedral intermediate formation. The second step, breakdown of the tetrahedral intermediate, also involves a barrier and solvent H_2O mediated proton transfer from the carbonyl end of the molecule to the nitrogen end. We have simulated this step with a single water to concertedly abstract and transfer the proton, but it is equally likely that an OH^- could abstract the proton and a different H_2O could deliver it to the amine. Even though the anomeric effect is important in determining the conformation of the tetrahedral complex (N lone pair app to C–O2 bond), it does not appear to be important in causing a *net* lowering of the barrier in solution.

Let us now critically assess the features of this approach. The use of ab initio theory at the SCF/MP2 level offers a powerful approach to studying the intrinsic energies of chemical reactions, provided of course that an adequate basis set can be used for the problem at hand. In the calculations presented here, the use of diffuse basis functions was crucial in reasonably representing the relative energies of reactants, tetrahedral intermediate, and products even in the gas phase. At the highest level of theory, the calculated gas-phase ΔE for reaction 1 was −48.9 kcal/mol, in agreement with the experimental enthalpy of −46.3 kcal/mol for this reaction.[35]

The second part of our approach involved a molecular mechanical calculation on the solvation of the various reactants, products, and intermediate steps along the hydrolysis reaction. We have evaluated $E_{int\ solute} + E_{solute-solvent}$ in two ways: the first involves adding quantum mechanical energies for $E_{int\ solute}$ to the solute–solvent interaction energy calculated by using molecular mechanical approaches. The second involves evaluating both $E_{int\ solute}$ and $E_{solute-solvent}$ by an alternate method which involves quantum mechanical calculations to include the electrostatic part of the solute–solvent interaction and classical calculations to determine solute–solvent van der Waals and polarization interactions. The fact that these two approaches gave rather similar results is encouraging and supports the use of simple molecular mechanical calculations to evaluate $E_{solute-solvent}$.

To evaluate $\Delta E_{solvent-solvent}$ upon introduction of the solute required a number of subjective decisions on how many waters to include in this calculation and how to determine the solvent–solvent energies. Our decision to include only those waters closer than the first minimum in the radial distribution to evaluate $\Delta E_{solvent-solvent}$ was due to the difficulty of consistently implementing any other model. Such an approach underestimates the absolute magnitude of $\Delta E_{solvent-solvent}$. This underestimate of solvent–solvent energy changes leads to absolute $\Delta H_{solvation}$ of OH^- (Table VII) too exothermic[37] by ≈34 kcal/mol. However, the approach seems to give reasonable relative values, such that the net calculated ΔE for reaction 1 in solution (−10.2 kcal/mol) is reasonably close to the experimental value (ΔH = −6 kcal/mol).

One of the reasons that these molecular mechanical (energy refinement) approaches to calculating solvation energies work at all is that the energies are dominated by very strong ionic interactions. Thus, the need for extensive averaging, inherent in much more time-consuming Monte Carlo and molecular dynamics approaches, is not so great. It has been our experience from Monte Carlo simulations on dimethylphosphate[38] that $E_{solute-solvent}$ converges relatively rapidly with such an approach but $\Delta E_{solvent-solvent}$ is much more time-consuming to accurately determine. To summarize, the weakest part of the approach presented here is the method for extracting $\Delta E_{solvent-solvent}$. By carrying out Monte Carlo or molecular dynamics calculations with periodic boundary conditions, one could avoid the problems of "edge effects" and a limited sampling of solvent–solvent energies. Thus, we plan to compare the results of our simpler model with the results of Monte Carlo or molecular dynamics solvation calculations on a number of the eight snapshot structures discussed above; the results of these more time-consuming calculations will be reported in due course. We stress, however, that our simpler molecular mechanical approach is faster (6 VAX 11–780 h/point vs. ≈100 h or more for Monte Carlo), gives qualitatively reasonable energies and physically reasonable solute–solvent hydrogen-bonding patterns, and is likely to be easier to extend to more complex systems than

(34) Gas-Phase ΔH_f; $\Delta H_f(OH^-)$ = −33.7 kcal/mol, ΔH_f ($HCONH_2$) = −44.5 kcal/mol, ΔH_f ($HCOO^-$) = −114.5, ΔH_f (NH_3) = −11.0 kcal/mol. NH_3 and OH^- from Wagman, D. "Selected Values of Thermodynamic Properties"; U.S. Government Printing Office: Washington DC, 1968. $HCONH_2$ from; Bander, A.; Gundhard, H. *Helv. Chim. Acta* **1958**, *41*, 670. $HCOO^-$ from thermodynamic cycle using ΔH_f (HCOOH), ΔH_f (H), ΔH_f (H^+), and ΔH_{rxn} ($HCOOH \rightarrow HCOO^- + H^+$); Yamdagni, R.; Kabarle, P. *J. Am. Chem. Soc.* **1975**, *95*, 4050. Cox; Pilcher In "Thermodynamics of Organic and Organometallic Compounds"; Academic Press: New York, 1970.

(35) Aqueous-phase ΔH_f; $\Delta H_f(OH^-)$ = −55.0 kcal/mol, $\Delta H_f(HCONH_2)$ = −60.7 kcal/mol, $\Delta H_f(HCOO^-)$ = −101.7, $\Delta H_f(NH_3)$ = −19.2 kcal/mol. Wagman, D. "Selected Values of Thermodynamic Properties": U.S. Government Printing Office: Washington, DC, 1968.

(36) Bunton, C.; Nayak, B.; O'Connor, C. *J. Org. Chem.* **1968**, *33*, 572.

(37) Friedman, H. L.; Krishnan, C. V. In "Water: A Comprehensive Treatise"; Franks, Ed.; Plenum Press: New York, 1973; Vol. 2.

(38) Alagona, G.; Ghio, C.; Kollman, P. *J. Am. Chem. Soc.*, in press.

Table IX. Solution-Phase Energetics for the Reaction: $Cl^- + CH_3Cl \rightarrow ClCH_3 + Cl^-$

struct[a]	$\Delta E(QM)$[b]	$\Delta E_{solute-solvent}$[c]	$\Delta\Delta E_{solvent-solvent}$[d]	$\Delta E_{solvation}$[e]	$\Delta E(MM)$[f]
react	0.0	0.0	0.0	0.0	0.0
bipyr	3.6	29.0	−9.2	19.8	23.4

[a] React. corresponds to the reactants separated at infinity: bipyr represents the bipyramidal transition state. [b] The difference in quantum mechanical energies for the two structures was taken from ref 39a. [c] Difference in calculated molecular mechanical solute–solvent interaction energy between the reactants and transition state by using the same approach as described for formamide/OH^- (kcal/mol). [d] Difference between calculated $\Delta E_{solvent-solvent}$ between the reactants and transition state by using the same approach as described for formamide/OH^- (kcal/mol). Since Chandrasekhar et al.[30] found a coordination number of Cl^- of 7, we took the seven waters closest to either Cl atom in each structure and evaluated their solvent–solvent energy. [e] $\Delta E_{solute-solvent} + \Delta\Delta E_{solvent-solvent}$ (kcal/mol). [f] $\Delta E(QM) + \Delta E_{solute-solvent} + \Delta\Delta E_{solvent-solvent}$ (kcal/mol).

are full Monte Carlo simulations. Alternatively, one could carry out an approach whereby very short molecular dynamics runs are used to "heat up" the system, followed by molecular mechanics energy refinement. In this way, molecular dynamics simulations would help "pop" the system out of local energy minima. The computer time would be greater than straight molecular mechanics but have the advantage of sampling more of the conformational space.

Upon submission of the original version of this manuscript, we were stimulated to further assess this approach for simulating reaction pathways involving ions in solution by the recent paper of Chandrasekhar et al.[39] who studied the S_N2 displacement reaction

$$Cl^- + CH_3Cl \rightarrow ClCH_3 + Cl^- \qquad (14)$$

by using a combination of ab initio quantum mechanics and Monte Carlo umbrella sampling methods. They calculated a gas-phase barrier of 2.4 kcal/mol, a solution phase $\Delta G^\ddagger = 26.3$ kcal/mol, and a solution $\Delta E^\ddagger = 29 \pm 8$ kcal/mol, in good agreement with the experimental $\Delta G^\ddagger = 26.6$ and $\Delta E^\ddagger = 23 \pm 3$ kcal/mol (ref 40). We used the geometry and Lennard-Jones and electrostatic parameters from the Chandrasekhar et al. study and our molecular mechanical solvation model on the reactants separated by 6.00 Å and on the pentagonal bypyramidal transition state. Table IX summarizes the results of our calculations, and the calculated $\Delta E^\ddagger = 23.4$ kcal/mol is in fortuitously good agreement with that of the more accurate calculations and experiment.

Thus, the fact that our approach can calculate reasonable relative energies for two rather different reactions suggests that the approach may work on other ionic chemical reactions. Our approach is less rigorous and accurate than that of Chandrasekhar et al. but can be more easily applied to complex systems and involves 1–2 orders of magnitude less computer time.

Our calculations determined the energy (enthalpy) of the reaction, whereas the analysis by Guthrie[22] focuses on the free energy. We expect there to be two major contributions to the entropy differences along the reaction pathway. First, the loss of translational and rotational entropy in forming the tetrahedral intermediate would stabilize both reactants and products relative to all intermediate points. Using molecular mechanics techniques,[41] we can estimate that the gas-phase $T\Delta S$ at 298 K for reactants → tetrahedral complex is −9.0 kcal/mol. It is more difficult to quantify this $T\Delta S$ contribution in solution, but it will almost certainly be negative and somewhat smaller in magnitude than in the gas phase. Second, a major contribution comes into play only in the solution reaction and is the solvent electrostriction due to ionic effects. Smaller anions such as OH^- will reduce the entropy of the surrounding H_2O molecules more than large, diffuse anions such as the intermediate structures in the reaction. The change in entropy upon solvation of OH^- is more negative than that of I^- by 26 eu at 298 K,[31] corresponding to a $T\Delta S$ of 7.7 kcal/mol. We see that this effect is of opposite sign as the loss of translational and rotational entropy change and of the same order of magnitude. Thus, it is reasonable to suppose that the calculated energy profile (Table IV) may be a reasonable approximation to the free energy profile for formamide hydrolysis.

A nice feature of the approach presented here is that it is straightforward to extend to complex enzyme–substrate–water systems, such as catalysis by the serine proteases.[42] Along these lines, we are currently carrying out combined quantum/molecular mechanical calculations on peptide hydrolysis in the active site of trypsin.[43] One of the features of the serine proteases that has intrigued enzymologists for some time has been the unusual reactivity of the serine OH in the enzyme, compared to an alcoholic OH, in hydrolyzing a peptide bond.[44] It is clear now that this reactivity is *not due* to the COO^- in the active site facilitating proton transfer from Ser 195 to Asp 102 through His 57.[45] We suggest that a substantial proportion of the cause of the unusual reactivity of this serine is that, once it has begun to deliver a proton to His 57 ($\Delta pK_a \approx 7$, $\Delta G \approx 10$ kcal/mol), the groups in the enzyme reduce the solvation of the incipient $R-O^-$ sufficiently to allow attack on the peptide bond without any further barrier (analogous to the gas-phase first step presented here), and the barrier to proton-transfer back to the substrate amine (formerly amide) NH_2 is also relatively facile (given the relative pK_a of these groups[46]). Thus, the role of desolvation by the enzyme of reactive or incipiently reactive groups should not be overlooked as a mechanism by which enzymes improve their catalytic efficiency over solution reactions. The importance of solvation in this regard has been stressed by Wolfenden,[47] and the calculations reported here and related approaches applied to enzyme catalysis as well as biomimetic models will be able to assess the role of solvation/desolvation vs. propinquity in specific cases.

Summary and Conclusions

We have presented the development of an ab initio quantum mechanical plus molecular mechanical approach to simulating complex reactive processes in the "gas phase" and in solution and have applied this approach to formamide hydrolysis by the hydroxide ion. In the gas phase, the first step, OH^- attack, involves no barrier, and water-catalyzed proton transfer to the amine (formerly amide) and accompanying peptide C–N bond cleavage has a ≈13 kcal/mol barrier. In solution, on the other hand, the first step involves a barrier of 22 kcal/mol while the barrier in the second step is little effected by solvation. The energetics of the reaction pathway calculated in solution and the gas phase and solution energies (enthalpies) for the overall reaction are quite consistent with available experimental data for these processes.

Note Added in Proof. We (Weiner[43] and Weiner, Serbel, and Kollman, unpublished) have confirmed the suggestion made above on the serine proteases by carrying out a combined quantum mechanical/molecular mechanical simulation of trypsin, 200 H_2O molecules, and an Ace-Phe-Val-Lys-Nme substrate. The calcu-

(39) (a) Chandrasekhar, J.; Smith, S.; Jorgensen, W. *J. Am. Chem. Soc.* **1985**, *107*, 154. (b) Chandrasekhar, J.; Smith, S.; Jorgensen, W. *J. Am. Chem. Soc.* **1984**, *106*, 3049.

(40) Bathgate, R.; Moelwyn-Hyghes, E. *J. Am. Chem. Soc.* **1959**, *81*, 2642.

(41) Hagler, A.; Stern, P.; Sharon, R.; Becker, J.; Naider, F. *J. Am. Chem. Soc.* **1979**, *101*, 6842.

(42) See: Kraut, J. *Annu. Rev. Biochem.* **1977**, *46*, 331.

(43) Weiner, S. Ph.D. Thesis, University of California at San Francisco, Dec. 1984.

(44) Blow, D. *Acc. Chem. Res.* **1976**, *9*, 145.

(45) Kossiakoff, A.; Spencer, S. *Nature (London)* **1980**, *288*, 414.

(46) Komiyama, M.; Bender, M. *Proc. Natl. Acad. Sci. U.S.A.* **1979**, *76*, 557.

(47) Wolfenden, R. *Science (Washington, DC)* **1983**, *222*, 1087.

lated reaction profile is somewhere between the gas phase and solution profiles represented in Figure 9.

Acknowledgment. We gratefully acknowledge Caterina Ghio who wrote the first version of the program to incorporate a solute "water bath" as an option in AMBER. We thank W. Jorgensen for sending us the Monte Carlo snapshot of 216 TIPS4P H_2O molecules and for sending us ref 39a prior to publication. This study was supported by NIH (GM-29072 to PAK). The U.C.S.F. computer graphics lab Evans and Sutherland Picture System 2 (supported by RR-1081, R. Langridge, director, and T. Ferrin system, manager) was very useful for displaying and analyzing all preliminary and refined structures. We thank J. Kirsch, W. Jencks, and J. Caldwell for their helpful discussions.

Registry No. Formamide, 75-12-7.

Monte Carlo Simulations of the Solvation of the Dimethyl Phosphate Anion

Giuliano Alagona,† Caterina Ghio,† and Peter A. Kollman*

Contribution from the Department of Pharmaceutical Chemistry, University of California, San Francisco, California 94143. *Received July 6, 1984*

Abstract: Monte Carlo (MC) simulations have been carried out for the (DMP) dimethyl phosphate anion $(CH_3O)_2PO_2^-$ in water, using TIPS2 and TIP4P potentials for the H_2O and analogous potentials for the anion. The simulations employed 216 H_2O molecules and 1 DMP, using periodic boundary conditions in an NPT ensemble. Preferential sampling and "umbrella sampling" techniques were employed to analyze the conformational dependence of anion solvation in H_2O. Analysis of the solvation energetics suggested a ΔE solvation for DMP of −65 to −95 kcal/mol, in reasonable agreement with expectations based on analogous small solutes. The partial molar volume of solvation of DMP is calculated to be ~60 cm^3/mol. Analysis of the water structure around DMP suggests four types of water: (1) those tightly bound to the $O^{\delta-}$; (2) H-bonding waters to the ester oxygen; (3) hydrophobically bound waters near the CH_3 group; and (4) bulk waters. The conformational dependence of the solvation has been analyzed in separate simulations on gauche,gauche (g,g) and gauche,trans (g,t) conformations.

One of the most challenging problems in simulations of complex molecules is the determination of an accurate representation of the effect of solvent on the properties of the molecules being studied. In the long term, the goal is to have an accurate description of the ensemble average properties of solute conformations and solvent configurations for a complete representation of the system.

There have been important advances in two avenues which lead us toward this goal. In the first, simulations of the conformations of macromolecules using molecular dynamical methods have begun to allow us to sample conformational heterogeneity in these molecules.[1] Much more recently, such simulations have been carried out, including the crystal environment.[2] Although such simulations only give us relatively short (subnanosecond) representations of macromolecular configurations, the development of Langevin dynamical methods to "average" over less important degrees of freedom and specialized computer hardware to use in simulations should allow significant progress toward the goal to be made in the near future.

The second avenue toward the goal has been to develop more precise models of water and aqueous solutions and to use this information to gain a new qualitative understanding of the nature of solvation as well as perhaps helping to create simple solvation models which can then be used in simulations of macromolecules.

Important progress in the development of models of water and aqueous solutions has been made because of the molecular dynamical simulations of Rahman and Stillinger[3] and the Monte Carlo simulations of Owicki and Scheraga,[4] Beveridge et al.,[5] Clementi,[6] Berne et al.,[7] Alagona and Tani,[8] and Jorgensen.[9] The above simulations have focused on the nature of water and very simple solutes, such as CH_4, Ar, Cl^-, and Na^+. These simulations have been more successful at describing the nature of water and the hydrophobic effect than they have been in accurately representing solvation energies. Monte Carlo and molecular dynamical simulations on more complex systems have also been illuminating. The papers of Rossky and Karplus[10] and Hagler et al.[11] have shown that one can derive interesting information on conformational dependent solvation energies on simulations of the alanyl dipeptide. More recently, the use of umbrella sampling techniques has allowed the simulation of the conformational equilibrium of *n*-butane in water.[12,13]

There have been important recent technical developments which should allow more accurate simulations of solvation energies and properties. Even though the initial Owicki and Scheraga papers used in the NPT ensemble,[4] this method has been much less used than the NVT method. Particularly in cases where the partial molar volume of solvation of a species is unknown, it seems more physically reasonable to carry out simulations in an NPT ensemble, which allows the volume of the system as well as its interparticle coordinates to change during the simulation, even though this costs a modest additional amount of computer time. Jorgensen has carried out a large number of simulations on water liquid and has determined potentials (TIPS2[14] and TIP4P[15]) which give an ex-

† Permanent address: Istituto di Chimica Quantistica ed Energetica Molecolare del C.N.R.—Via Risorgimento 35, 56100 Pisa, Italy.

(1) Karplus, M.; McCammon J. A. *Annu. Rev. Biochem.* **1983**, *52*, 263.
(2) von Gunsteren, W. F.; Berendsen, H. J. C.; Hermans, J.; Hol, W. G.; Postma, J. P. M. *Proc. Natl. Acad. Sci. U.S.A.* **1983**, *80*, 4315.
(3) Stillinger, F. H.; Rahman, A. *J. Chem. Phys.* **1974**, *60*, 1545.
(4) (a) Owicki, J. C.; Scheraga, H. A. *J. Am. Chem. Soc.* **1977**, *99*, 7403. (b) *Ibid.* **1977**, *99*, 7413.
(5) (a) Swaminathan, S.; Beveridge, D. L. *J. Am. Chem. Soc.* **1977**, *99*, 8392. (b) Swaminathan, S.; Harrison, S. W.; Beveridge, D. L. *Ibid.* **1978**, *100*, 5705.
(6) Clementi, E. "Liquid Water Structure"; Springer Verlag: New York, 1976 and references cited therein.
(7) Pangali, C.; Rao, M.; Berne, B. J. *Chem. Phys. Lett.* **1978**, *55*, 413.
(8) Alagona, G.; Tani, A. *J. Chem. Phys.* **1980**, *72*, 580.
(9) Jorgensen, W. L. *J. Am. Chem. Soc.* **1979**, *101*, 2016; **1981**, *103*, 335.
(10) Rossky, P. J.; Karplus, M. *J. Am. Chem. Soc.* **1979**, *101*, 1913.
(11) Hagler, A. T.; Osguthorpe, D. J.; Robson, B. *Science Washington, D. C.* **1980**, *208*, 599.
(12) Rosenberg, R. O.; Mikkilineni, R.; Berne, B. J. *J. Am. Chem. Soc.* **1982**, *104*, 7647.
(13) Jorgensen, W. L. *J. Chem. Phys.* **1982**, *77*, 5757.
(14) (a) Jorgensen, W. L. *J. Chem. Phys.* **1982**, *77*, 4156. (b) Chandrasekhar, J.; Jorgensen, W. L. *J. Chem. Phys.* **1982**, *77*, 5080.

0002-7863/85/1507-2229$01.50/0